Regulation and roles of the hyaluronan system in mammalian reproduction

Omnia Mohey-Elsaeed [A] , Waleed F. A. Marei [B D], Ali A. Fouladi-Nashta [C] and Abdel-Aleem A. El-Saba [A]

[A] Department of Cytology and Histology, Faculty of Veterinary Medicine, Cairo University, Giza 12211, Egypt.

[B] Department of Theriogenology, Faculty of Veterinary Medicine, Cairo University, Giza 12211, Egypt.

[C] Department of Comparative Biomedical Sciences, Royal Veterinary College, Hatfield AL9 7TA, UK.

[D] Corresponding author. Email: wmarei@staff.cu.edu.eg

Abstract

We investigated the local modulation of some histochemical properties of oviducts of the dromedary (Camelus dromedarius), focusing on the immnolocalisation of hyaluronic acid (HA) synthases (HAS2 and HAS3), hyaluronidases (HYAL2 and HYAL1) and the HA receptor CD44 in the ampulla and isthmus. Abundant acidic mucopolysaccharides (glycosaminoglycans) were detected by Alcian blue staining along the luminal surface of both ciliated and non-ciliated epithelial cells (LE). Staining for HAS2 was higher in the primary epithelial folds of the ampulla compared with the isthmus, especially in secretory cells, adluminal epithelial surface and supranuclear cell domain. HAS3 staining was stronger in the LE of the isthmus than ampulla. HYAL2 was detected in the LE in the ampulla and isthmus and was more intense in the adluminal projections of secretory cells. HYAL1 was weakly detected in the LE with no difference between the ampulla and isthmus. Strong CD44 immunostaining was present in the LE of the ampulla and isthmus. CD44 staining was higher in secretory cells than in ciliated epithelial cells and was higher in the supranuclear region than the basal region of the cytoplasm. In conclusion, we provide evidence that HA synthesis and turnover occur in the camel oviduct. Differences in HAS2 and HAS3 expression suggest regional differences in the molecular size of HA secreted in oviductal fluid that may influence oviduct–gamete interaction in the camel.

Introduction

The oviduct is a highly specialised 'reproductive organ' (Menezo and Guerin 1997) in which many reproductive events take place, such as sperm transport and capacitation, oocyte transport and fertilisation, and early embryo development and transport to the uterus. Most of these events are regulated by the secretory function of oviductal lining epithelium that contributes to oviductal secretion with various materials that provide a suitable microenvironment for these events to occur. Some of the functions of the oviduct are also regulated by direct interaction between gametes and oviductal epithelial cells. The oviduct is divided into three regions: the infundibulum, ampulla and isthmus. After sperm transport and capacitation in the isthmus and ovum pick up by the infundibulum, fertilisation occurs in the ampulla (Hawk 1987). These regional roles require and suggest specific regional micromorphology and function, and adjustments in the biochemical composition of the oviductal fluid. Differences in protein and glycoprotein composition of oviductal secretions between the ampulla and isthmus were observed many years ago (Nieder and Macon 1987; Buhi et al. 1990). Explanted sections of ampulla of the oviduct, but not explants from the isthmus or uterus, were able to support mouse embryonic development (Whittingham 1968). These findings suggest that gradient changes in the oviductal microenvironment are required to facilitate specific roles for each region. Knowledge of these differences should provide scientific bases for the development of assisted reproductive technologies; however, to date, little is known in this regard.

Oviductal fluid contains a vast number of components that may influence oviduct–gamete interactions and support early embryo development. Avilés et al. (2010) listed more than 160 different components of the oviductal fluid that are required for optimal development of the different processes that take place in the oviduct. Among those factors, oviductal glycans are of special interest. Glycosaminoglycans have received little research attention despite evidence of their critical role during oocyte maturation (Teixeira Gomes et al. 2009; Marei et al. 2012; Raheem et al. 2013) and embryo development (Marei et al. 2013).

Hyaluronic acid (HA), a non-sulfated glycosaminoglycan, is a major constituent of the extracellular matrix (ECM) abundant in most tissues and is also present in body fluids. HA can be found in oviductal (Tienthai et al. 2000) and uterine (Teixeira Gomes et al. 2009; Raheem et al. 2013) fluids. There is increasing evidence that HA is not only present as a space filler, but is also involved in various biological functions that involve binding to specific receptors and initiation of cell signalling. It is also evident that the function of HA is highly dependent on its molecular weight (Toole 2004). HA is a linear polymer composed of repeating disaccharides of glucouronic acid and N-acetyl glucosamine synthesised by the HA synthases HAS1, HAS2 and HAS3 (Spicer et al. 1997). These synthases are located at the inner

surface of the plasma membrane (Prehm 1984) and extrude the growing polymer chain through the membrane into the pericellular space (Weigel et al. 1997). Each HAS is characterised by a different molecular stability and average length (molecular size) of the HA produced (Dougherty and van de Rijn 1993; Crater and van de Rijn 1995; Itano and Kimata 2002; Stern 2005).

HA has an extraordinary high turnover rate. HA is degraded by a family of enzymes named hyaluronidases (HYALs). HYAL1 and HYAL2 are the most common HYALs in somatic cells (Csoka et al. 2001). HYAL2 breaks down high molecular weight HA into 20–30 kDa fragments but has no effect on low molecular weight HA fragments (Lepperdinger et al. 1998).

The major cell surface receptor for HA is a membrane glycoprotein called CD44, which has high binding affinity for HA (Aruffo et al. 1990). The ability of a single molecule of HA to bind to multiple CD44 receptor sites (Underhill 1992) enables the involvement of this receptor in cell–cell and cell–ECM interactions, adhesion and migration (Lesley et al. 1993). CD44–HA interactions also mediate endocytosis of exogenous HA, leading to its degradation by lysosomal HYAL1 (McCourt 1999). CD44–HA interactions are also known to initiate cell signalling, which induces cytokine secretion, stimulates expression of growth factor receptors, protects against apoptosis and enhances cell proliferation and cell motility (Stern et al. 2006).

The dromedary, also known as the Arabian camel, is an important livestock in many countries, including Egypt, in addition to its economic importance in tourism and camel races in some countries. Assisted reproduction in camels is still challenging compared with cattle because camels are characterised by late puberty, seasonal breeding and induced ovulation (Ismail 1987; Skidmore 2003). Most IVF, capacitation, fertilisation and embryo transfer procedures are extrapolated from cattle and can be optimised for camel oocytes and semen. Studying the histochemical characteristics and HA system in the camel oviduct could provide some basic knowledge required for the development of assisted reproductive technologies in this species. This may also have some application in other species.

The present study was performed to investigate the local modulation of some histochemical properties in the ampulla and isthmus regions of the oviduct during the breeding season of the camel, focusing on immunohistochemical changes of HA system (HAS, HYALs and CD44).

Materials and methods

Sample Collection

Reproductive tracts of adult female camels (Camelus dromedarius; n = 5) were collected from a local abattoir during the breeding season. Tracts with ovaries containing a large anovulatory follicle (1–1.9 cm in diameter) were selected. Ipsilateral oviducts were immediately dissected from the surrounding connective tissue and from the uterus. Sections from the ampulla (1–3 cm from the infundibulum) and isthmus (1–2 cm from the uterotubal junction) were immediately fixed in 10% buffered formalin for 48 h. Tissues were then rinsed and kept in 70% ethanol until processing and embedding in paraffin blocks.

Histological and histochemical examination

Tissue blocks were cut into 5-µm sections, mounted on glass slides and left to dry. Sections were rehydrated through a series of decreasing concentrations of ethanol. General histological structure was examined by haematoxylin and eosin (H&E) staining or Crossman trichrome staining following conventional protocols (Bancroft and Stevens 1982). Some sections were stained using the periodic acid-Schiff (PAS) reaction to examine neutral mucopolysaccharides or with Alcian blue (pH 2.5) to locate acidic mucopolysaccharides (Bancroft and Stevens 1982).

Localisation of the HA system by immunohistochemistry

Protein expression of HAS2, HAS3, HYAL1, HYAL2 and the HA receptor CD44 was determined by immunohistochemistry (IHC) as described previously (Raheem et al. 2013), with some modifications. Briefly, paraffin-embedded oviductal sections (5 µm) mounted on superfrost slides were used. Antigen retrieval was performed for 30 min in boiling sodium citrate (2.947 g L–1, pH 6.0). Non-specific binding was blocked using 10% (v/v) normal horse serum (Dako, Glostrup, Denmark) and 4% (w/v) bovine serum albumin (BSA) in phosphate-buffered saline (PBS) for 45 min. Endogenous peroxidase was blocked using hydrogen peroxide 3% v/v in methanol for 30 min. Primary antibodies used for immunostaining were polyclonal rabbit anti-HAS2 (1 : 100; Sc-66916; Santa Cruz Biotechnology, Santa Cruz, CA, USA), polyclonal rabbit anti-HAS3 (1 : 100; Sc-66917; Santa Cruz Biotechnology), HYAL1 (1 : 200; HPA002112; Sigma, St Louis, MO, USA); HYAL2 (1 : 100; AB90004; Abcam, Cambridge, UK) and monoclonal mouse anti-CD44v6 (1 : 200; MCA1730; AbD Serotec, Kidlington, UK). Simultaneously, sections for negative controls were treated in the same way but replacing primary antibody with normal rabbit or normal mouse IgGs (Santa Cruz Biotechnology) at the same concentrations. The reaction was completed with horseradish peroxidase-conjugated polyclonal swine anti-rabbit secondary antibody (1 : 200; P0217; Dako) or rabbit anti-mouse (1 : 200; P0260; Dako) and visualised using diaminobenzidine (DAB; Vector Laboratories, Peterborough, UK). Nuclei were counterstained with haematoxylin and differentiated using acid alcohol. Slides were examined under a light microscope (DM500; Leica, Wetzlar, Germany) and images were captured using an attached digital camera (ICC50 HD; Leica).

Semiquantitative analysis of immunostaining

Immunostaining was assessed semiquantitatively using histochemical score (HSCORE) as described previously (Ponglowhapan et al. 2008). Briefly, the HSCORE was calculated by multiplying the intensity (as a score of 0–3) of the brown DAB stain in a particular layer within the oviduct and the percentage of that area stained (0–100%). The estimate was based on five random fields per section from five different oviducts. Images were scored by two independent experienced assessors blinded to the corresponding region.

Statistical analysis

Numerical data generated by HSCORE are summarised as the mean ± s.e.m. T-tests were used to compare HSCOREs of the ampulla and isthmus using SPSS version 21 (IBM SPSS Statistics for Windows, Version 21.0. Armonk, NY: IBM Corp.). Two-tailed T-test at $P < 0.05$ was considered significant.

Results

Histology of the camel oviduct

The wall of the camel oviduct appeared to consist of mucosa, submucosa, muscularis and outermost serosa layers (Fig. 1). The mucosa of the ampulla consisted of large and numerous primary folds that branched, forming secondary folds and sometimes tertiary folds (Fig. 1a). The epithelium was mainly simple columnar ciliated and non-ciliated (secretory or peg) cells (Fig. 1b). The ciliated cells contained oval or ovoid basally situated basophilic nuclei containing fine chromatin granules. Some of the columnar ciliated cells were vacuolated. Peg cells were narrower than ciliated cells and characterised by dome-shaped cytoplasmic projections protruding from the apical (luminal) surface (Fig. 1b–d). The nuclei of peg cells were basal, elongated and flattened laterally, containing dense chromatin granules. Morphological signs of secretory activity were evident in peg cells that possessed more deeply stained cytoplasm by H&E and a vesicular and basally situated nucleus (Fig. 1b). Peg cells were also strongly positive to PAS stain, indicating the presence of abundant neutral polysaccharides (Fig. 1c), and also contained fine alcianophilic granules, especially in the supranuclear region and the apical cytoplasmic projection as seen by Alcian blue staining (Fig. 1d), indicating the presence of acidic polysaccharides.

The epithelium was separated from the lamina propria submucosa with a PAS-positive basement membrane (Fig. 1c). The lamina propria submucosa was formed of a thin layer under the epithelium and extended into the mucosal folds (Fig. 1e). It consisted of loose connective tissue (CT) and sometimes contained a few leucocytes and small blood vessels. The CT of the lamina propria was denser in the primary and secondary folds and less dense in the tertiary folds (Fig. 1a, f).

The tunica muscularis of the ampulla consisted mainly of inner circular and thin outer longitudinally arranged smooth muscle fibres (Fig. 1e) that were positive to PAS (Fig. 1g).

The serosa consisted of loose CT with many blood vessels and some dispersed circular and longitudinal bundles of smooth muscle fibres. The serosa was covered externally with simple squamous mesothelium (Fig. 1h, i). The dispersed muscle bundles and the tunica intima of the arterioles in the lamina propria and serosa were positive to PAS (Fig. 1g).

In the isthmus, the lumen was narrower than that of the ampulla with fewer primary folds and very few secondary folds (Fig. 2a). The epithelium appeared to be high columnar to pseudostratified columnar epithelium containing ciliated and non-ciliated cells as well as basal cells. (Fig. 2b–e). The non-ciliated peg cells were less abundant and protruded less into the lumen compared with in the ampulla. The reaction of these cells towards Alcian blue stain was restricted to the apical surface (Fig. 2d). Peg cells were also positive to PAS staining (Fig. 2e). The basal cells appeared triangular, faintly stained with rounded nuclei (Fig. 2b).

The lamina propria was similar to that of the ampulla, whereas the tunica muscularis was very thick, consisting of several alternating layers of circular and longitudinal smooth muscles (Fig. 2f–h). The isthmus was covered by serosa composed of highly vascularised loose CT and mesothelium (Fig. 2a).

Immunolocalisation of HAS2

HAS2 immunostaining in the ampulla and isthmus was detected in the lamina epithelialis (LE), muscularis, blood vessels and mesothelium of the serosa, whereas the lamina propria and CT of the serosa were negative (Fig. 3a–g). In the LE of the ampulla, the intensity of HAS2 immunostaining was moderate in the peripheral (primary) folds (Fig. 3a–c). Staining was stronger in the adluminal epithelial surface and the supranuclear cell domain than in the basal cell compartment, and some nuclei were strongly stained (Fig. 3b). Expression of HAS2 in secondary and tertiary folds of the LE in the ampulla (Fig. 3c) and isthmus (Fig. 3e, f) was less than in primary folds of the ampulla (Fig. 3i). Some nuclei were weakly stained. Expression of HAS2 in peg cells was relatively higher than in ciliated epithelial cells, particularly in the dome-shaped part in the lumen in the ampulla. It was noted that HAS2 staining was also strong at the mesothelium covering the serosa (Fig. 3f, g). Negative controls revealed no immunostaining or background (Fig. 3h).

Immunolocalisation of HAS2

HAS3 immunostaining in ciliated and secretory cells of the LE of the isthmus was moderate and relatively stronger compared with the LE of the ampulla, where HAS3 immunostaining was mainly restricted to peg cells. The lamina propria was strongly stained in the ampulla, but not in the isthmus. Moderate staining was also detected in the inner layer of the tunica muscularis in both the ampulla and isthmus, whereas less intense staining in the outer layers was observed (Fig. 4a–d, g). HAS3 staining was also detectable in the CT in the serosa (Fig. 4b, e). No immunostaining or background was detected in negative controls (Fig. 4f).

Immunolocalisation of HYAL2

HYAL2 was detected in LE cells in the ampulla (Fig. 5a) and isthmus (Fig. 5b) and was more intense in the adluminal projections of peg cells (Fig. 5c, d), which were more abundant in the ampulla. HYAL2 was weak in the lamina propria, moderate in the musculosa and serosa, and strong at the mesothelium. No staining could be detected in the negative controls (Fig. 5e). There were no significant differences in the localisation and intensity of HYAL2 staining between the ampulla and isthmus (Fig. 5f).

Immunolocalisation of HYAL1

HYAL1 immunostaining was detected in the LE (Fig. 6) with no difference between the ampulla and isthmus (Fig. 6a, b). Very weak HYAL1 staining was also observed in the lamina propria and musculosa. A negative control is shown in Fig. 6c.

Immunolocalisation of CD44

Strong CD44 immunostaining was present in the LE of the ampulla and isthmus. CD44 staining was higher in peg cells than ciliated epithelial cells and was higher in the supranuclear region than in the basal region of the cytoplasm (Fig. 7a–d). CD44 immunostaining was high in the muscular layer as well as in the smooth muscles of the blood vessels of the serosa and in the mesothelial lining of the serosa (Fig. 7a, b). CD44 immunostaining was weak in the propria submucosa, but the fibrocytes were strongly stained (Fig. 7d). This pattern of expression was similar to the pattern of PAS-positive staining shown in the ampulla (Fig. 1c, g) and isthmus (Fig. 2e). A negative control is shown in Fig. 7e. There were no significant differences in the HSCORE of CD44 staining intensity between the ampulla and isthmus in different layers (Fig. 7f).

Discussion

The aim of the present study was to examine the histochemical properties of the camel oviduct, focusing on the immnolocalisation of HAS, HYALs and the HA receptor CD44 in the ampulla and isthmus regions. In the camel, the follicular cycle can be divided into a growth phase (~10 days), a mature phase (~8 days) and a regression phase (~12 days; Skidmore et al. 1996). For the purpose of the present study, oviducts ipsilateral to ovaries carrying dominant follicles ranging between 1 and 1.9 cm in diameter were selected. This follicular size has been shown previously to correspond with the optimum time for mating because it is associated with the highest ovulation rates following mating or buserelin injection (Skidmore et al. 1996).

The results of the present study show that the histological structure of the oviduct is similar to that described before in the camel (Srikandakumar et al. 2011; Accogli et al. 2014) and other ruminants (Abe 1996). Oviductal epithelium consists of a single layer of ciliated and non-ciliated columnar cells (Srikandakumar et al. 2011). We observed that the epithelial cells were taller in the isthmus compared with the ampulla and that non-ciliated peg cells were characterised by dome-shaped projections on the luminal surface, particularly in the ampulla. These ‘apical blebs’ of peg cells have been described in camel oviducts as a typical feature of the mature phase of the oestrous cycle associated with the apocrine pattern of oviductal secretion (Accogli et al. 2014).

Plasma membranes of epithelial cells are organised into two distinct domains: the apical domain, which faces the lumen, and the basolateral domain, which includes the rest of the cell (Wang and Margolis 2007). These domains are separated by a ring of tight junctions, have different protein compositions and are targets of different types of Golgi vesicles (Wang and Margolis 2007). These differences may explain some of the differences in histochemical properties and immunolocalisation of HA-related proteins in the LE of the ampulla and isthmus of the camel oviduct, as discussed below.

We found that PAS and Alcian blue positive staining in the LE was restricted to the secretory cells, particularly to the adluminal projections in both the ampulla and isthmus. This indicates the presence of neutral and acidic polysaccharides in the oviductal secretions in the camel. This is in accordance with a previous report in the camel (Accogli et al. 2014). Numerous glycoconjugates were also reported in lama oviduct, some of which were shown to play a role in sperm binding to oviductal epithelium (Apichela et al. 2010). Among the acidic polysaccharides that are positively stained by Alcian blue, glycosaminoglycans, particularly HA, are of special interest because of their role in fertilisation and embryo development. For this reason, we focused on the immunolocalisation of the HA system in the ampulla and isthmus of the camel oviduct.

HAS2 is known to produce high molecular weight (HMW) HA (>2 × 103 kDa), whereas HAS3 produces 0.1–1 × 103 kDa HA (Stern et al. 2006). We examined HAS expression in camel oviducts using immunohistochemistry to determine localisation within different layers of the oviduct at the ampulla and isthmus. We found that HAS2 and HAS3 are expressed in the LE in both ciliated and secretory cells. The expression of HAS2 in the LE was highest in the primary folds of the ampulla compared with the isthmus, whereas HAS3 expression was higher in the isthmus than ampulla. This suggests regional differences in the size of HA. There is growing evidence that HA plays a role in sperm transport, capacitation, fertilisation and embryo development in many species, including cattle, sheep and pigs (Tienthai et al. 2003a). Regional differences in the molecular size of HA in the ampulla and isthmus may be required to regulate the role of HA in these events. The intensity of immunostaining for both HAS2 and HAS3 was relatively higher in secretory cells compared with ciliated cells, and higher in the adluminal epithelial surface and the supranuclear cell domain. This indicates that HA is secreted from secretory cells as a constituent of oviductal fluid, and is also produced by ciliated cells, perhaps to play a role in the interaction between the LE and gametes or embryo. This observation is reinforced by abundant acidic mucopolysaccharides (glycosaminoglycans) detected by Alcian blue staining along the apical (luminal) surface of both ciliated and non-ciliated epithelial cells. In a previous report, the mRNA for HAS2 and HAS3 was

shown to be expressed in the bovine oviduct during the oestrous cycle (Ulbrich et al. 2004) and although no significant differences could be detected between the ampulla and isthmus, the density of electrophoresis bands fro the HAS3 polymerase chain reaction (PCR) product was stronger in the isthmus than ampulla. This was based on a whole-tissue homogenate and not representative of a particular layer. In the same study, the relative intensity of the HA (detected using HA-binding protein) appeared to be greater in the ampulla than in the isthmus (Ulbrich et al. 2004). This suggests differences in the molecular weight of HA between the ampulla and isthmus in other species.

We found differences in HAS2 and HAS3 expression in other layers of the oviduct. The CT of the lamina propria extending in oviductal folds and surrounding the mucosa, as well as serosa, was negative for HAS2 but strongly positive for HAS3. In human and porcine oviducts (Edelstam et al. 1991; Tienthai et al. 2000), bovine oviducts (Ulbrich et al. 2004) and bovine endometrium (Raheem et al. 2013), hyaluronan has been localised to the entire lamina propria surrounding the LE and extending into oviductal villi. The detection of HAS but not HA in the LE suggests that HA produced by LE is directly secreted into oviductal fluid and thus lost during tissue processing for staining. We found that HAS2 is weakly detected in the lamina propria and HAS3 is predominant, which suggests that HA in the lamina propria is derived primarily from HAS3. It is also worth noting that we observed positive HAS2 staining in some nuclei of the LE. HAS are localised at the plasma membrane; thus, nuclear staining seems perplexing. In a previous study, HAS1 immunostaining was found in nuclei of different layers of ovine endometrium (Raheem et al. 2013).

HA is a non-sulfated glycosaminoglycan. Another glycosaminoglycan, heparin, is found in oviductal fluid (Bergqvist and Rodriguez-Martinez 2006) and was shown to be potent in maintaining sperm motility and triggering capacitation in vitro in cattle (Parrish et al. 1994). It has been shown recently that HA plays an important role during oocyte maturation (Marei et al. 2012) and preimplantation embryo development (Marei et al. 2013). Of the different HA receptors, CD44 is a widely distributed cell-surface receptor and is considered the main receptor for HA. In swine, exogenous HA improved development of parthenogenetic embryo development in vitro (Toyokawa et al. 2005). This was suggested to be mediated through a cellular response via CD44 because the effects of HA were abolished in the presence of anti-CD44 antibodies (Toyokawa et al. 2005). In that study, the authors also claimed that exogenous HA is accessible to its own receptor through the zona pellucida in order to serve as a ligand. In the present study, we found that CD44 is expressed in LE cells in the ampulla and isthmus. The intensity of CD44 staining was highest at the surface membrane and supranuclear domain of mainly secretory cells. The apical cell surface localisation of CD44 corresponds to the cell

membrane HA receptor, and the supranuclear localisation may represent the internalised CD44. This pattern of expression is very similar to that described previously in the lining epithelium of the porcine oviduct (Tienthai et al. 2003b). In contrast, there was no evidence of epithelial staining of CD44 in bovine oviducts using anti-porcine CD44 monoclonal antibody (Ulbrich et al. 2004). We could not detect any significant difference in CD44 immunostaining between the ampulla and isthmus. In contrast, in bovine oviduct, the mRNA expression of CD44 was found to be >10-fold higher in the isthmus than ampulla (Ulbrich et al. 2004). However, because this expression is derived from a whole-region transcript, the overall higher CD44 in the isthmus may be due to thicker muscle layers that strongly express CD44.

The ligand-binding properties of CD44 are modulated by alternative splicing, creating CD44 variant (CD44v) isoforms. The antibodies used to detect CD44 in the present study were specific for the CD44v6 splice variant. On the basis of studies of tumour progression and metastatic potential, CD44 encoded by variant exon 6 (v6) is thought to be necessary for efficient HA adhesion (Menzel and Farr 1998). Thus, expression of this variant on the LE of camel oviducts suggests that CD44 can efficiently bind HA and may mediate HA functions in the oviduct. Interactions between HA and CD44 and other hyaladherins create a complex, hydrated microenvironment that supports and promotes the cellular characteristics of proliferating and migrating cells (Toole 2004). CD44 also mediates a variety of intracellular signalling cascades and interacts with cytoskeletal proteins that are essential for the normal functioning of the cells.

HYAL1 and HYAL2 are the most abundant HYALs in somatic cells. HYAL2 is located on the cell surface colocalised with CD44 and depolymerises HMW HA into fragment of 20–30 kDa in size. HYAL1 is a lysosomal enzyme that degrades HA after internalisation by CD44 into tetra- and oligosaccharides (Underhill 1992). It is important to note that we found HYAL2 to be expressed in a very similar pattern to CD44 in the LE. HYAL2 is known to be colocalised with CD44 on the cell membrane. Depolymerisation of extracellular HMW HA bound to CD44 into smaller fragments results in disruption of HA–CD44 interactions, which initiates CD44 signalling (Ohno-Nakahara et al. 2004). HYAL2 was also been shown to be expressed in bovine oviducts and the addition of HYAL2 to bovine embryo culture in vitro enhanced embryo cell proliferation and resulted in better-quality embryos (Marei et al. 2013). In addition, in the present study we detected weak immunostaining for HYAL1 in the LE of the camel oviduct; HYAL1 is required for lysosomal degradation of HA after internalisation by CD44. Intracellular HA fragments are biologically active and can bind to other receptors like receptor for hyaluronan-mediated motility (RHAMM). These small-size HA fragments have been associated with the induction of cytokine synthesis (Termeer et al. 2002; Shimada et al. 2008) and

upregulation of heat shock protein expression (Xu et al. 2002) and thus may influence embryo–maternal interaction.

In conclusion, we provide evidence that enzymes required for HA synthesis and turnover are expressed in the camel oviduct. Differences in HAS2 and HAS3 expression suggest regional differences in HA molecular size. The HA receptor CD44 is also expressed in the LE of the ampulla and isthmus. HA–CD44 interactions are suggested to be involved in oviduct–gamete interactions in the camel.

330 **References**

331 Abe, H. (1996). The mammalian oviductal epithelium: regional variations in cytological and functional
332 aspects of the oviductal secretory cells. Histol. Histopathol. 11, 743–768.

333 Accogli, G., Monaco, D., El Bahrawy, K. A., El-Sayed, A. A., Ciannarella, F., Beneult, B., Lacalandra, G.
334 M., and Desantis, S. (2014). Morphological and glycan features of the camel oviduct epithelium. Ann.
335 Anat. 196, 197–205.

336 Apichela, S. A., Valz-Gianinet, J. N., Schuster, S., Jimenez-Diaz, M. A., Roldan-Olarte, E. M., and Miceli,
337 D. C. (2010). Lectin binding patterns and carbohydrate mediation of sperm binding to llama oviductal
338 cells in vitro. Anim. Reprod. Sci. 118, 344–353.

339 Aruffo, A., Stamenkovic, I., Melnick, M., Underhill, C. B., and Seed, B. (1990). CD44 is the principal cell
340 surface receptor for hyaluronate. Cell 61, 1303–1313.

341 Avilés, M., Gutiérrez-Adán, A., and Coy, P. (2010). Oviductal secretions: will they be key factors for the
342 future ARTs? Mol. Hum. Reprod. 16, 896–906.

343 Bancroft, J. D., and Stevens, A. (1982). 'Theory and practice of histological techniques.' 2nd edn.
344 (Churchill Livingstone: Edinburgh.)

345 Bergqvist, A. S., and Rodriguez-Martinez, H. (2006). Sulphated glycosaminoglycans (S-GAGs) and
346 syndecans in the bovine oviduct. Anim. Reprod. Sci. 93, 46–60.

347 Buhi, W. C., Alvarez, I. M., Sudhipong, V., and Dones-Smith, M. M. (1990). Identification and
348 characterization of de novo-synthesized porcine oviductal secretory proteins. Biol. Reprod. 43, 929–
349 938.

350 Crater, D. L., and van de Rijn, I. (1995). Hyaluronic acid synthesis operon (HAS) expression in Group A
351 streptococci. J. Biol. Chem. 270, 18 452–18 458.

352 Csoka, A. B., Frost, G. I., and Stern, R. (2001). The six hyaluronidase-like genes in the human and mouse
353 genomes. Matrix Biol. 20, 499–508.

354 Dougherty, B. A., and van de Rijn, I. (1993). Molecular characterization of hasB from an operon
355 required for hyaluronic acid synthesis in Group A streptococci. Demonstration of UDP-glucose
356 dehydrogenase activity. J. Biol. Chem. 268, 7118–7124.

357 Edelstam, G. A., Lundkvist, O. E., Wells, A. F., and Laurent, T. C. (1991). Localization of hyaluronan in
358 regions of the human female reproductive tract. J. Histochem. Cytochem. 39, 1131–1135.

359 Hawk, H. W. (1987). Transport and fate of spermatozoa after insemination of cattle. J. Dairy Sci. 70,
360 1487–1503.

361 Ismail, S. T. (1987). A review of reproduction in the female camel (Camelus dromedarius).
362 Theriogenology 28, 363–371.

363 Itano, N., and Kimata, K. (2002). Mammalian hyaluronan synthases. IUBMB Life 54, 195–199.

364 Lepperdinger, G., Strobl, B., and Kreil, G. (1998). HYAL2, a human gene expressed in many cells,
365 encodes a lysosomal hyaluronidase with a novel type of specificity. J. Biol. Chem. 273, 22 466–22 470.

366 Lesley, J., Hyman, R., and Kincade, P. W. (1993). CD44 and its interaction with extracellular matrix.
367 Adv. Immunol. 54, 271–335.

368 Marei, W. F., Ghafari, F., and Fouladi-Nashta, A. A. (2012). Role of hyaluronic acid in maturation and
369 further early embryo development of bovine oocytes. Theriogenology 78, 670–677.

370 Marei, W. F., Salavati, M., and Fouladi-Nashta, A. A. (2013). Critical role of hyaluronidase-2 during
371 preimplantation embryo development. Mol. Hum. Reprod. 19, 590–599.

372 McCourt, P. A. (1999). How does the hyaluronan scrap-yard operate? Matrix Biol. 18, 427–432.

373 Menezo, Y., and Guerin, P. (1997). The mammalian oviduct: biochemistry and physiology. Eur. J.
374 Obstet. Gynecol. Reprod. Biol. 73, 99–104.

375 Menzel, E. J., and Farr, C. (1998). Hyaluronidase and its substrate hyaluronan: biochemistry, biological
376 activities and therapeutic uses. Cancer Lett. 131, 3–11.

377 Nieder, G. L., and Macon, G. R. (1987). Uterine and oviducal protein secretion during early pregnancy
378 in the mouse. J. Reprod. Fertil. 81, 287–294.

379 Ohno-Nakahara, M., Honda, K., Tanimoto, K., Tanaka, N., Doi, T., Suzuki, A., Yoneno, K., Nakatani, Y.,
380 Ueki, M., Ohno, S., Knudson, W., Knudson, C. B., and Tanne, K. (2004). Induction of CD44 and MMP
381 expression by hyaluronidase treatment of articular chondrocytes. J. Biochem. 135, 567–575.

382 Parrish, J. J., Susko-Parrish, J. L., Uguz, C., and First, N. L. (1994). Differences in the role of cyclic
383 adenosine 3',5'-monophosphate during capacitation of bovine sperm by heparin or oviduct fluid. Biol.
384 Reprod. 51, 1099–1108.

385 Ponglowhapan, S., Church, D. B., and Khalid, M. (2008). Differences in the expression of luteinizing
386 hormone and follicle-stimulating hormone receptors in the lower urinary tract between intact and
387 gonadectomised male and female dogs. Domest. Anim. Endocrinol. 34, 339–351.

388 Prehm, P. (1984). Hyaluronate is synthesized at plasma membranes. Biochem. J. 220, 597–600.

389 Raheem, K. A., Marei, W. F., Mifsud, K., Khalid, M., Wathes, D. C., and Fouladi-Nashta, A. A. (2013).
390 Regulation of the hyaluronan system in ovine endometrium by ovarian steroids. Reproduction 145,
391 491–504.

392 Shimada, M., Yanai, Y., Okazaki, T., Noma, N., Kawashima, I., Mori, T., and Richards, J. S. (2008).
393 Hyaluronan fragments generated by sperm-secreted hyaluronidase stimulate cytokine/chemokine
394 production via the TLR2 and TLR4 pathway in cumulus cells of ovulated COCs, which may enhance
395 fertilization. Development 135, 2001–2011.

396 Skidmore, J. A. (2003). The main challenges facing camel reproduction research in the 21st century.
397 Reprod. Suppl. 61, 37–47.

398 Skidmore, J. A., Billah, M., and Allen, W. R. (1996). The ovarian follicular wave pattern and induction
399 of ovulation in the mated and non-mated one-humped camel (Camelus dromedarius). J. Reprod. Fertil.
400 106, 185–192.

401 Spicer, A. P., Seldin, M. F., Olsen, A. S., Brown, N., Wells, D. E., Doggett, N. A., Itano, N., Kimata, K.,
402 Inazawa, J., and McDonald, J. A. (1997). Chromosomal localization of the human and mouse
403 hyaluronan synthase genes. Genomics 41, 493–497.

404 Srikandakumar, A., Johnson, E. H., Mahgoub, O., Kadim, I. T., and Al-Ajmi, D. S. (2011). Anatomy and
405 histology of the female reproductive tract of the arabian camel. Emir. J. Agric. Sci. 13, 23–26.

406 Stern, R. (2005). Hyaluronan metabolism: a major paradox in cancer biology. Pathol. Biol. (Paris) 53,
407 372–382.

408 Stern, R., Asari, A. A., and Sugahara, K. N. (2006). Hyaluronan fragments: an information-rich system.
409 Eur. J. Cell Biol. 85, 699–715.

410 Teixeira Gomes, R. C., Verna, C., Nader, H. B., dos Santos Simoes, R., Dreyfuss, J. L., Martins, J. R.,
411 Baracat, E. C., de Jesus Simoes, M., and Soares, J. M. (2009). Concentration and distribution of
412 hyaluronic acid in mouse uterus throughout the estrous cycle. Fertil. Steril. 92, 785–792.

413 Termeer, C., Benedix, F., Sleeman, J., Fieber, C., Voith, U., Ahrens, T., Miyake, K., Freudenberg, M.,
414 Galanos, C., and Simon, J. C. (2002). Oligosaccharides of hyaluronan activate dendritic cells via Toll-
415 like receptor 4. J. Exp. Med. 195, 99–111.

416 Tienthai, P., Kjellen, L., Pertoft, H., Suzuki, K., and Rodriguez-Martinez, H. (2000). Localization and
417 quantitation of hyaluronan and sulfated glycosaminoglycans in the tissues and intraluminal fluid of
418 the pig oviduct. Reprod. Fertil. Dev. 12, 173–182.

419 Tienthai, P., Kimura, N., Heldin, P., Sato, E., and Rodriguez-Martinez, H. (2003a). Expression of
420 hyaluronan synthase-3 in porcine oviducal epithelium during oestrus. Reprod. Fertil. Dev. 15, 99–105.

421 Tienthai, P., Yokoo, M., Kimura, N., Heldin, P., Sato, E., and Rodriguez-Martinez, H. (2003b).
422 Immunohistochemical localization and expression of the hyaluronan receptor CD44 in the epithelium
423 of the pig oviduct during oestrus. Reproduction 125, 119–132.

424 Toole, B. P. (2004). Hyaluronan: from extracellular glue to pericellular cue. Nat. Rev. Cancer 4, 528–
425 539.

426 Toyokawa, K., Harayama, H., and Miyake, M. (2005). Exogenous hyaluronic acid enhances porcine
427 parthenogenetic embryo development in vitro possibly mediated by CD44. Theriogenology 64, 378–
428 392.

429 Ulbrich, S. E., Schoenfelder, M., Thoene, S., and Einspanier, R. (2004). Hyaluronan in the bovine
430 oviduct: modulation of synthases and receptors during the estrous cycle. Mol. Cell. Endocrinol. 214,
431 9–18.

432 Underhill, C. (1992). CD44: the hyaluronan receptor. J. Cell Sci. 103, 293–298.

433 Wang, Q., and Margolis, B. (2007). Apical junctional complexes and cell polarity. Kidney Int. 72, 1448–
434 1458.

435 Weigel, P. H., Hascall, V. C., and Tammi, M. (1997). Hyaluronan synthases. J. Biol. Chem. 272, 13 997–
436 14 000.

437 Whittingham, D. G. (1968). Development of zygotes in cultured mouse oviducts. I. The effect of varying
438 oviductal conditions. J. Exp. Zool. 169, 391–397.

439 Xu, H., Ito, T., Tawada, A., Maeda, H., Yamanokuchi, H., Isahara, K., Yoshida, K., Uchiyama, Y., and Asari,
440 A. (2002). Effect of hyaluronan oligosaccharides on the expression of heat shock protein 72. J. Biol.
441 Chem. 277, 17 308–17 314.
442

Fig. 1. Representative images showing the histological structure of the ampulla of the camel oviduct stained by (a, b, e, h, i) haematoxylin and eosin, (c, g) periodic acid-Schiff (PAS), (f) Crossman trichrome and (d) Alcian blue. The ampulla consisted of the lamina epithelialis (LE), lamina propria submucosa (LP), lamina muscularis (M) and outermost serosa (S). The LE and the underlining LP were highly folded into primary folds (1°), branching into secondary (2°) and tertiary (3°) folds. The LE consisted of secretory cells (Sec; black arrowheads) and non-secretory epithelial cells (Cil; black arrows). Some epithelial cells were vacuolated (V). Secretory cells (Sec) were positive for PAS (dark purple colour) and Alcian blue (blue colour). The serosa (S) was covered by mesothelium (Mes). Scale bars = 200 µm.

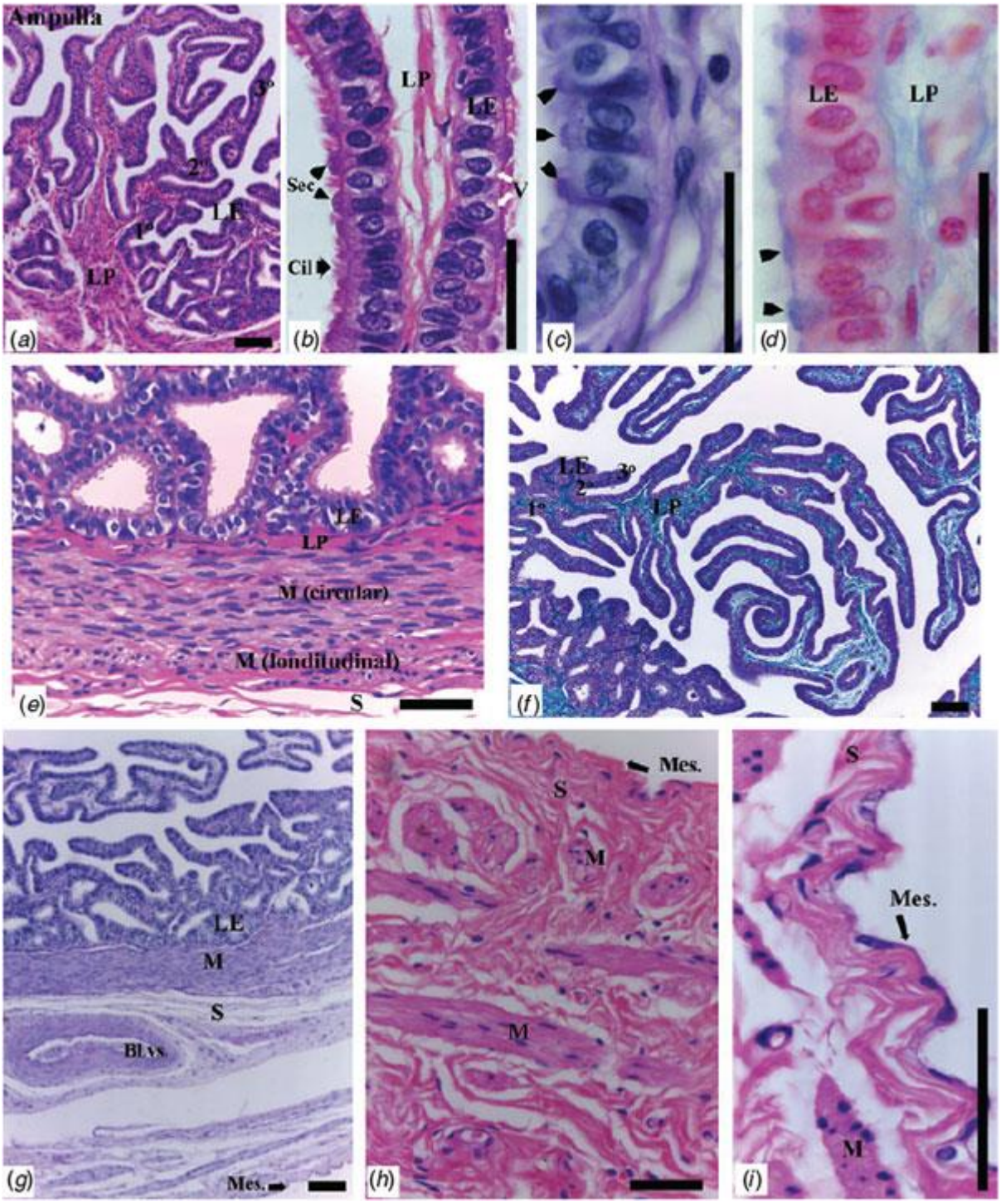

Fig. 2. Representative images showing histological structure of the isthmus of camel oviduct stained by (a, c, f, g) haematoxylin and eosin, (e) periodic acid-Schiff (PAS), (b, h) Crossman trichrome and ((d) Alcian blue. LE, lamina epithelialis; LP, lamina propria submucosa; M, lamina muscularis; S, outermost serosa; arrowheads, secretory cells (Sec); Cil, ciliated cells; L, C, layers of longitudinal and circular muscles, respectively; Bl.vs., blood vessels. Scale bars = 200 µm.

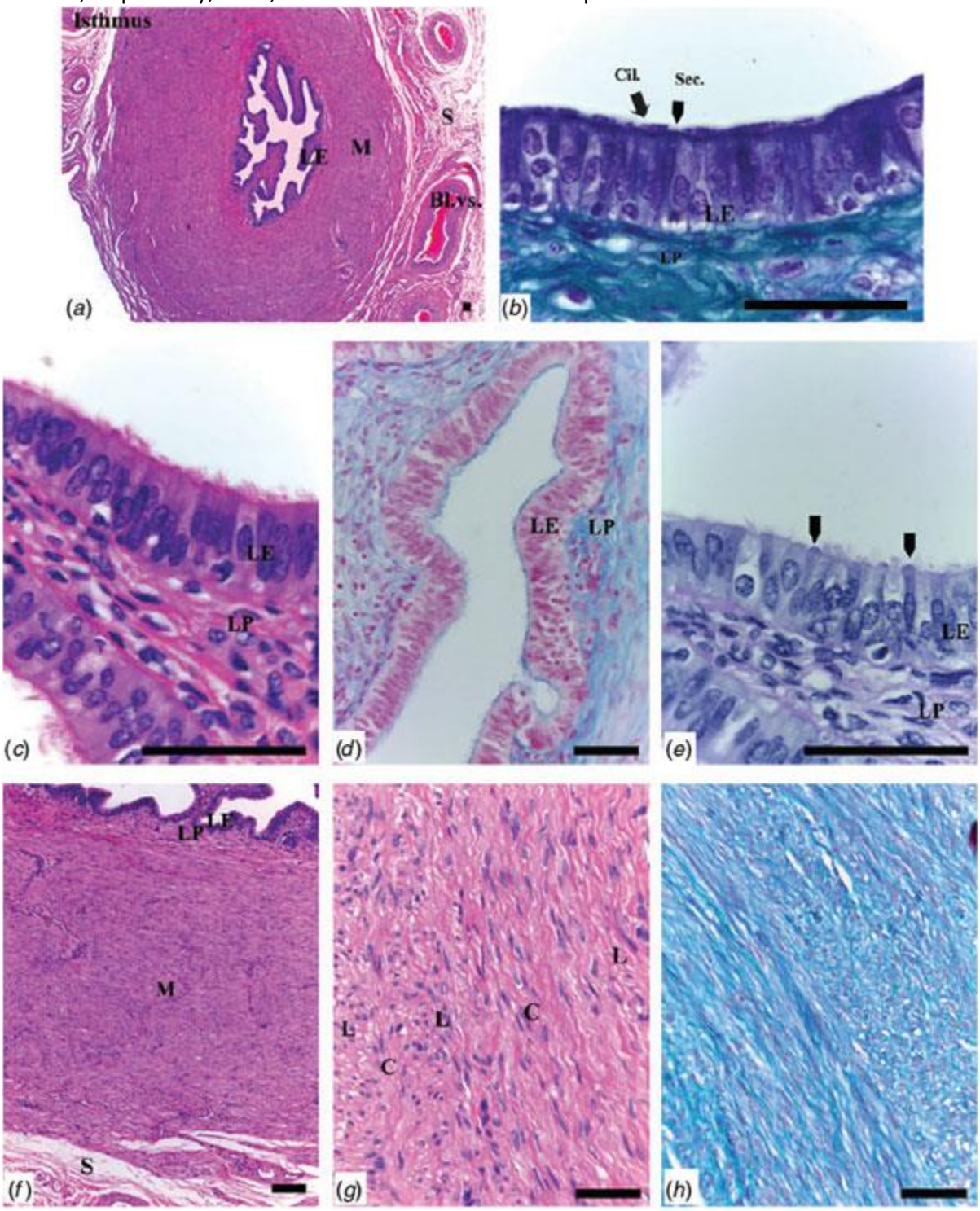

Fig. 3. Immunolocalisation of hyaluronic acid synthase (HAS) 2 in the (a–d) ampulla and (e–g) isthmus of the camel oviduct. HAS2 is shown as brown staining (diaminobenzidine), whereas nuclei are counterstained with haematoxylin (blue). (h) Negative control using normal rabbit IgG. LE, lamina epithelialis; LP, lamina propria submucosa; M, lamina muscularis; S, outermost serosa containing connective tissue (CT) and muscle bundles (M) and covered by mesothelium (Mes). 1°, 2°, 3°, primary, secondary and tertiary folds of the mucosa in the ampulla, respectively; arrowheads, secretory cells (Sec). Scale bars = 200 µm. (i) HSCORE for HAS2 immunostaining in different layers of the ampulla and isthmus. Data are the mean ± s.e.m. *P < 0.05.

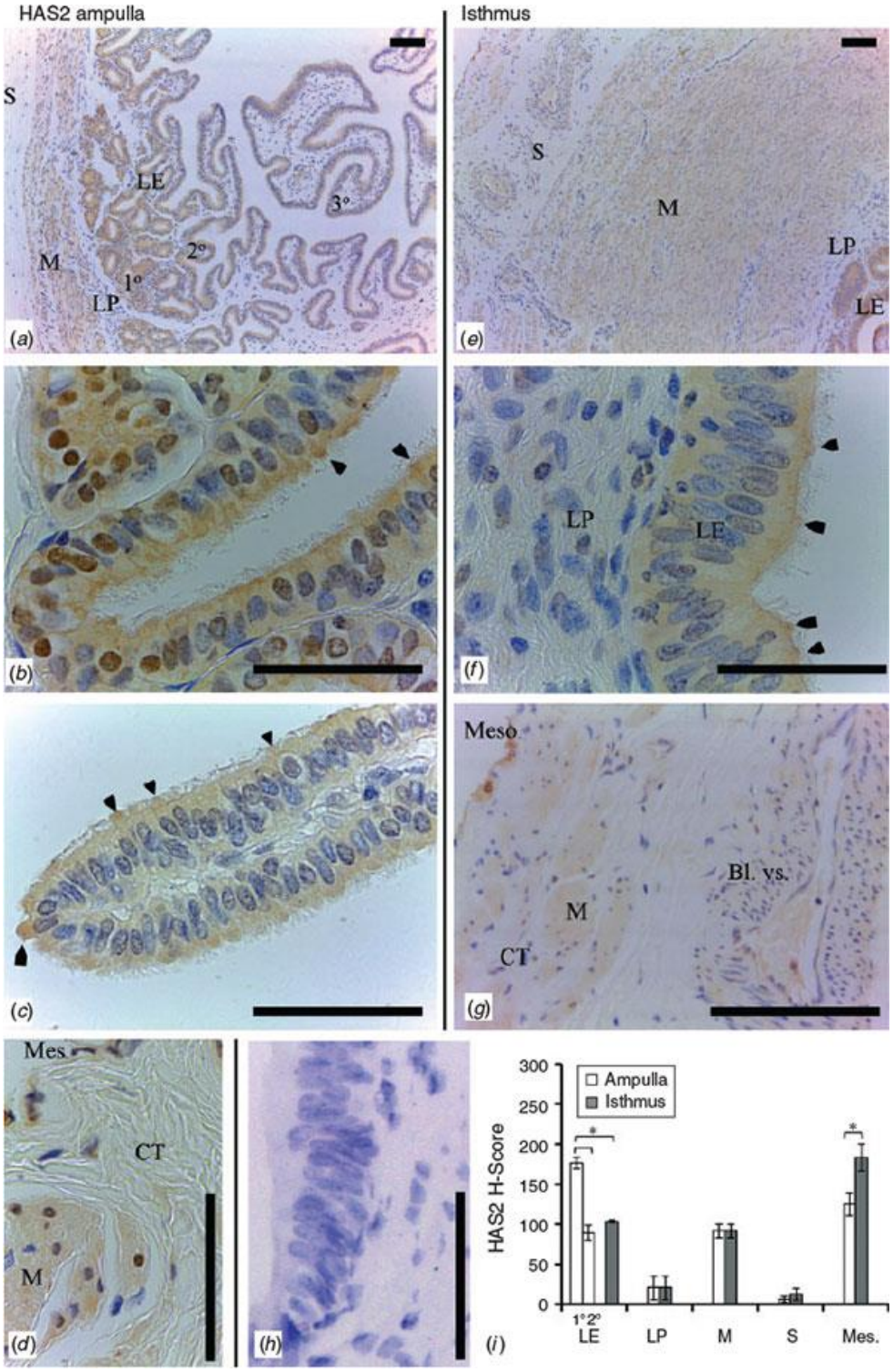

Fig. 4. Immunolocalisation of hyaluronic acid synthase (HAS) 3 in the (a, c) ampulla and (b, d, e) isthmus of the camel oviduct. (f) Negative control using normal rabbit IgG. HAS3 is shown as brown staining (diaminobenzidine), whereas nuclei are counterstained with haematoxylin (blue). LE, lamina epithelialis; LP, lamina propria submucosa; M, lamina muscularis; S, outermost serosa containing blood vessels (Bl.vs.) and covered by mesothelium (Mes); 1°, 2°, 3°, primary, secondary and tertiary folds of the mucosa in the ampulla, respectively; arrowheads, secretory cells (Sec). Scale bars = 200 µm. (g) HSCORE for HAS3 immunostaining in different layers of the ampulla and isthmus. Data are the mean ± s.e.m. *P < 0.05.

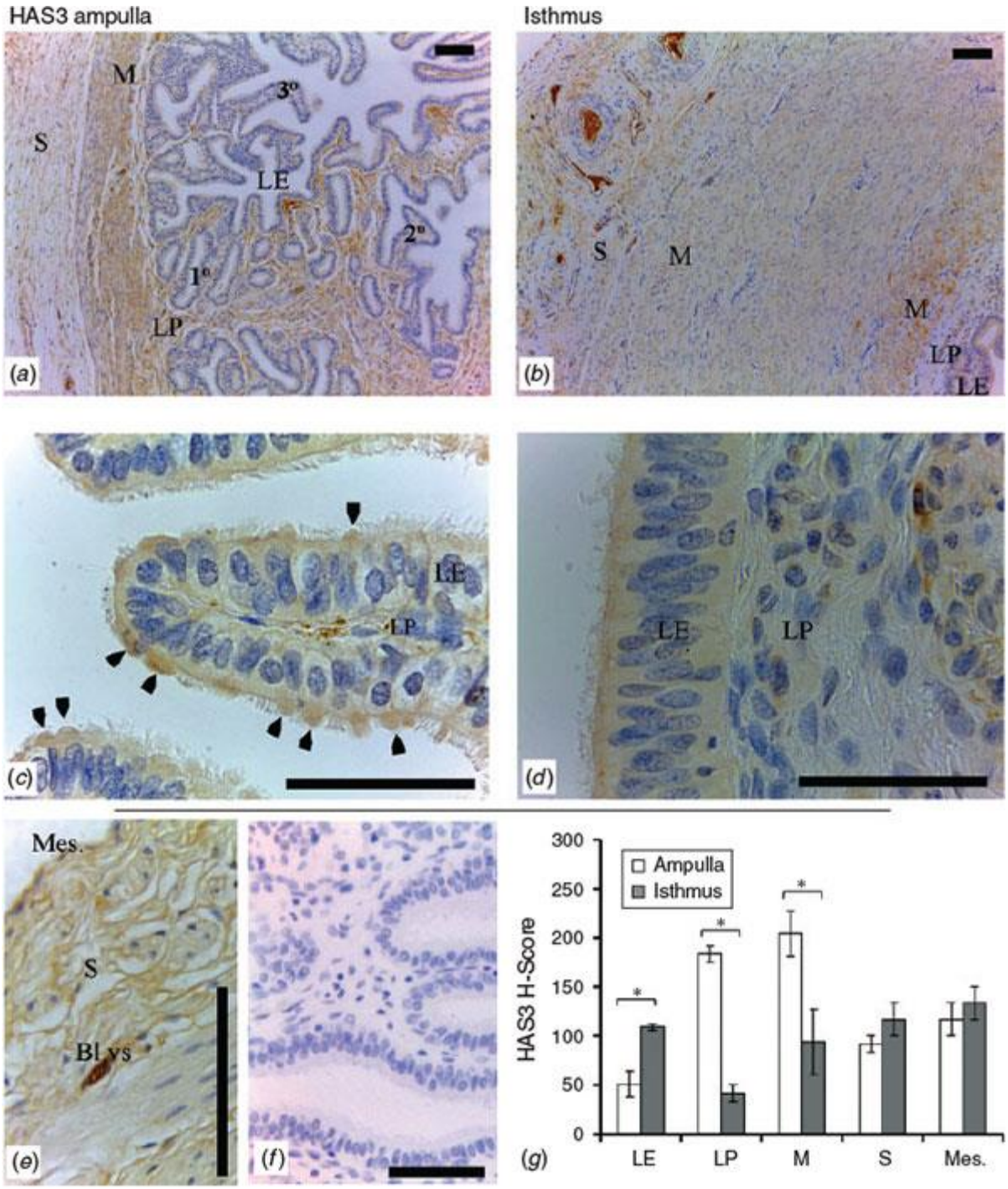

Fig. 5. Immunolocalisation of hyaluronidase (HYAL) 2 in the (a, c) ampulla and (b, (d) isthmus of the camel oviduct. HYAL2 is shown as brown staining (diaminobenzidine), whereas nuclei are counterstained with haematoxylin (blue). (e) Negative control using normal rabbit IgG. LE, lamina epithelialis; LP, lamina propria submucosa; M, lamina muscularis; S, outermost serosa; 1°, 2°, 3°, primary, secondary and tertiary folds of the mucosa in the ampulla, respectively; arrowheads, secretory cells (Sec). Scale bars = 200 µm. (f) HSCORE for HYAL2 immunostaining in different layers of the ampulla and isthmus. Data are the mean ± s.e.m. No significant differences were detected at $P < 0.05$.

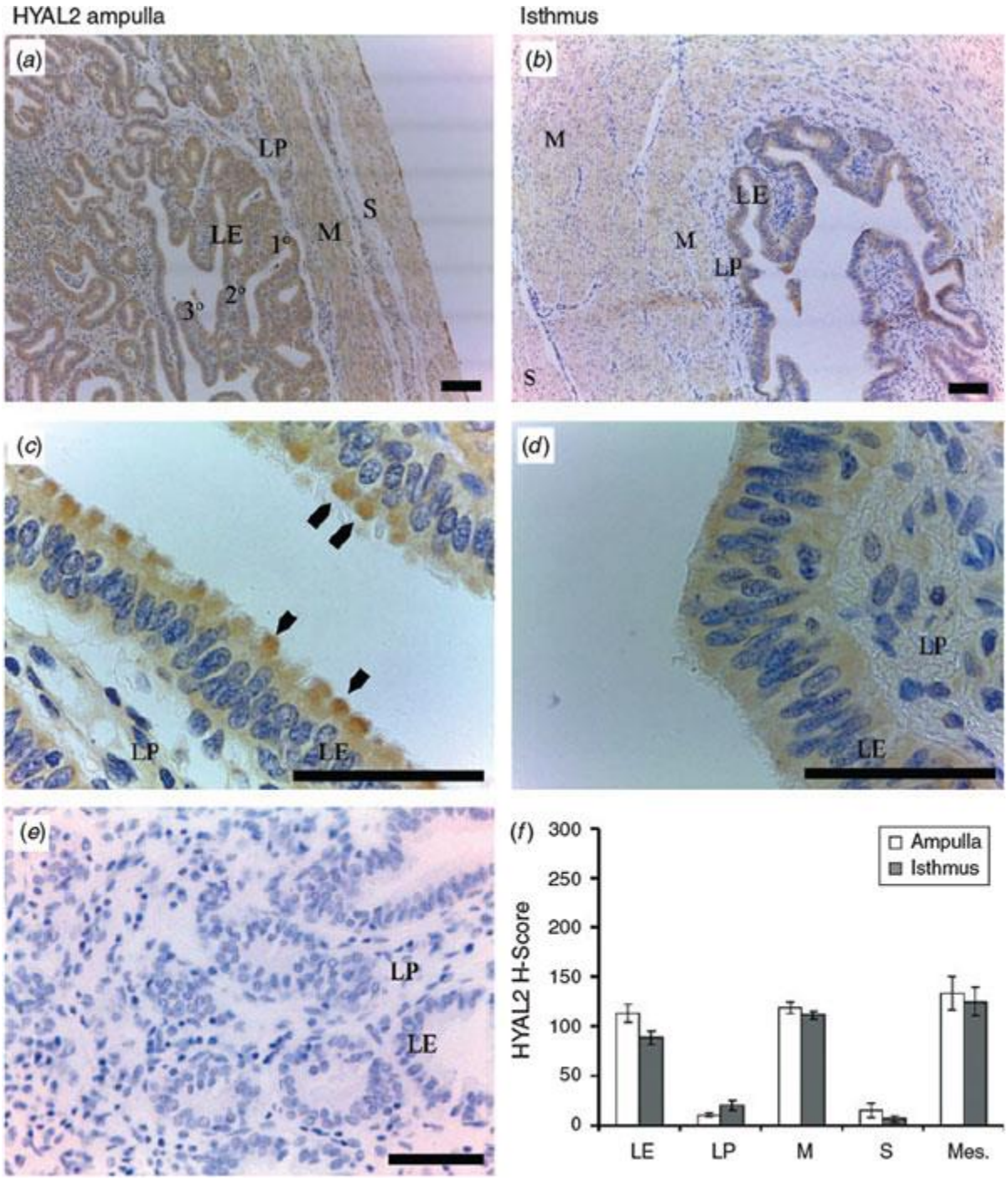

Fig. 6. Immunolocalisation of hyaluronidase (HYAL) 1 in the (a) ampulla and (b) isthmus of the camel oviduct. HYAL1 is shown as brown staining (diaminobenzidine) while nuclei are counterstained with haematoxylin (blue). (c) Negative control using normal rabbit IgG. LE, lamina epithelialis; LP, lamina propria submucosa; M, lamina muscularis. Scale bars = 200 µm.

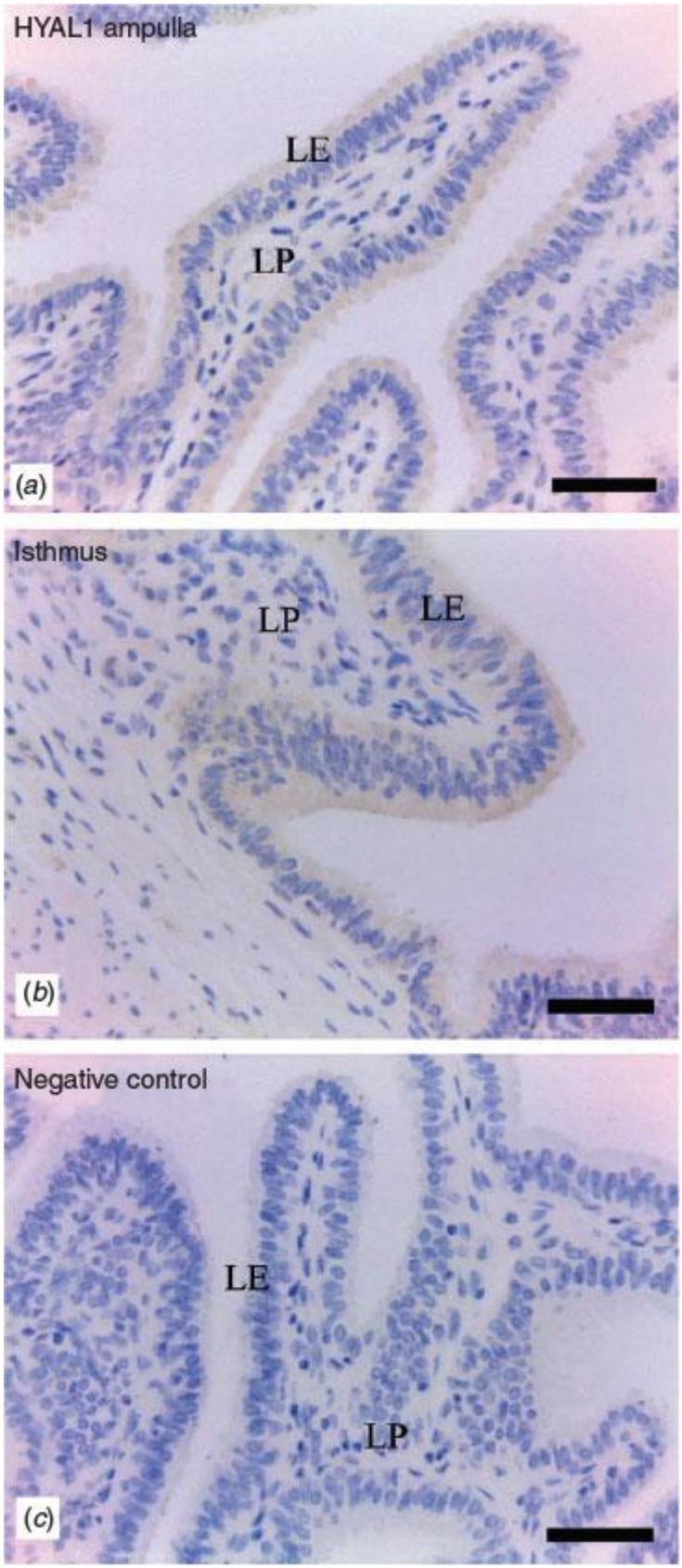

Fig. 7. Immunolocalisation of CD44v6 in the (a, c) ampulla and (b, (d) isthmus of the camel oviduct. CD44v6 is shown as brown staining (diaminobenzidine), whereas nuclei are counterstained with haematoxylin (blue). (e) Negative control using normal mouse IgG. LE, lamina epithelialis; LP, lamina propria submucosa; M, lamina muscularis; S, outermost serosa; 1°, 2°, 3°, primary, secondary and tertiary folds of the mucosa in the ampulla, respectively; arrowheads, secretory cells (Sec); F, fibrocytes. Scale bars = 200 µm. (f) HSCORE for CD44v6 immunostaining in different layers of the ampulla and isthmus. Data are the mean ± s.e.m. No significant differences were detected at P < 0.05.